Directed Motion of Proteins along Tethered Polyelectrolytes

Katja Henzler,[1] Sabine Rosenfeldt,[1] Alexander Wittemann,[1] Ludger Harnau,[2] Stephanie Finet,[3] Theyencheri Narayanan,[3] and Matthias Ballauff[1,*]

[1]*Physikalische Chemie I, University of Bayreuth, 95440 Bayreuth, Germany*

[2]*Max-Planck-Institut für Metallforschung, Heisenbergstrasse 3, D-70569 Stuttgart, Germany, and Institut für Theoretische und Angewandte Physik, Universität Stuttgart, Pfaffenwaldring 57, D-70569 Stuttgart, Germany*

[3]*ESRF, B.P. 220, 38043 Grenoble Cedex, France*

(Received 15 November 2007; published 14 April 2008)

We present the first time-resolved investigation of motions of proteins in densely grafted layers of spherical polyelectrolyte brushes. Using small-angle x-ray scattering combined with rapid stopped-flow mixing, we followed the uptake of bovine serum albumin by poly(acrylic acid) layer with high spatial and temporal resolution. We find that the total amount of adsorbed protein scales with time as $t^{1/4}$. This subdiffusive behavior is explained on the basis of directed motion of the protein along the polyelectrolyte chains.

DOI: 10.1103/PhysRevLett.100.158301 PACS numbers: 82.35.Rs, 87.15.Vv

The adsorption and immobilization of proteins from aqueous solutions onto solid surfaces is among the most important problems in biochemical research. Many biotechnological processes require immobilization of enzymes with full retention of their biological activity [1–4]. Reversible adsorption of proteins onto charged surfaces is involved in protein purification by ion exchange chromatography [5] and in many natural processes such as cell adhesion [3]. On the other hand, unspecific adsorption of proteins must be suppressed in many practical applications in order to prevent biofouling [6]. Very often, charged and uncharged polymers attached to surfaces are used to tune the interaction with proteins. Tethered chains of poly(ethylene oxide) are now widely used to prevent protein adsorption [7] while polyelectrolyte multilayers [8,9] or dense layers of polyelectrolytes [9–11] are utilized to immobilize proteins on surfaces.

Despite numerous studies, little is known about the kinetics of protein adsorption and the self-organization of biomolecules with tethered polymer chains on a molecular level. Evidently, the kinetics of protein adsorption plays a major role in these processes [4,5,8,10–13] and it is necessary to determine the position of the protein molecules on a molecular scale as a function of time. In this letter, we demonstrate for the first time that protein adsorption can be monitored directly with high temporal and spatial resolution on surface-modified colloidal spheres. We present the first study of the motion of a protein in a layer of tethered polyelectrolyte chains of a spherical polyelectrolyte brush [14] using time-resolved small-angle x-ray scattering (TR-SAXS) [15].

Figure 1 schematically displays a colloidal particle composed of poly(styrene) spheres with chemically grafted chains of poly(acrylic acid). The grafting of the polyelectrolyte chains is dense, with the average distance of the chains on the surface much smaller than their contour length L_c resulting in a spherical polyelectrolyte brush (SPB) [14]. The radius R of the cores of the SPB is 46 nm ($\sigma_R = 4\%$) and the thickness of the shell L is 58 nm ($\sigma_L = 25\%$). Here we study the spontaneous adsorption of bovine serum albumin (BSA). Despite the fact that both the SPB as well as the protein carry an overall negative charge, proteins can spontaneously adsorb onto these SPBs [12] at low ionic strength without inducing denaturation. Moreover, the biological activity of the bound and redesorbed proteins and enzymes is nearly the same as in the native state [12]. Hence, spherical polyelectrolyte brushes present a well-defined model system for the study of protein adsorption [12].

BSA solutions (15 g/l; Sigma A6003; Lot.: 045K7422) were prepared in a MES-buffer (2-*N*-morpholinoethane sulfonic acid) containing 2 m*M* NaN_3 to avoid microbial growth. The rather high concentration of the protein was necessary since the protein solution is diluted in the stopped-flow device. Moreover, much smaller concentrations would render the diffusion of the proteins to the surface of the particles the rate-limiting step. The pH was kept at 6.1 which is well above the isoelectric point of BSA (5.1) and the ionic strength in the solution was adjusted to 7 mM in order to ensure full uptake of BSA by the SPB. TR-SAXS experiments were performed at the beamline ID2 of the European Synchrotron Radiation Facility (ESRF, Grenoble, France) [15]. Solutions of BSA (15 g/l in MES-buffer) were mixed rapidly with aqueous suspensions of the SPB (2 wt. % in MES-buffer; number density: $4.23\ 10^{16} L^{-1}$) using a stopped-flow apparatus (BioLogic) described elsewhere [15]. The incident X-ray wavelength (λ) was 0.1 nm. In order to cover a wide scattering vector ($q = (4\pi/\lambda)\sin(\theta/2)$, with θ the scattering angle) range, SAXS intensities were recorded at two sample-detector distances of 2 m and 8 m by a high sensitive CCD detector (FReLoN). To obtain the optimal time resolution, the

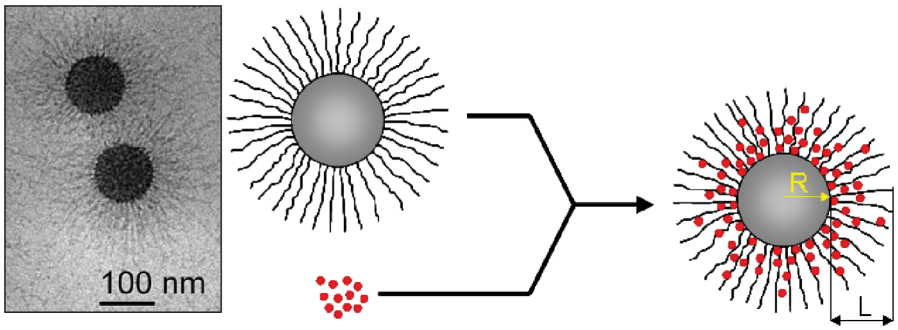

FIG. 1 (color). Schematic representation of the uptake of proteins by spherical polyelectrolyte brushes. These particles consist of a solid polystyrene core onto which long chains of the weak polyelectrolyte poly(acrylic acid) are grafted. In salt-free solutions, the polyelectrolyte chains are strongly stretched due to the high osmotic pressure of the confined counterions. This can be seen directly in the cryogenic transmission electron micrograph shown on the left-hand side [14]. Solutions of the spherical polyelectrolyte brushes in salt-free solution are rapidly mixed with aqueous solutions of the protein BSA. The uptake of the protein by the brush layer is monitored by time-resolved small-angle x-ray scattering.

exposure time for each SAXS pattern was 20 ms separated by a readout gap of 140 ms (4×4 binning) and the data acquisition was triggered after the mixing phase ($t \approx 0$).

The analysis of SAXS intensity as a function of time provides the information about the amount and the position of the proteins within the polyelectrolyte layer [16]. The background subtracted intensity $I(q)$ can be split into the intensity $I_0(q)$ of a single particle and the structure factor $S(q)$ describing the mutual interaction between particles:

$$I(q) = \frac{N}{V} I_0(q) S(q), \tag{1}$$

where N/V is the number of dispersed particles per volume. $S(q)$ can be obtained by an interaction site integral equation theory [17] that models the repulsive interaction between SPB. $I_0(q)$ of the SPB involves two parts, namely, $I_{CS}(q)$ that describes the core-shell structure of the particle and a second term $I_{fluct}(q)$ that takes into account the additional scattering contribution from the density fluctuations of the polyelectrolyte layer [16]. $I_{CS}(q) = B^2(q)$, where $B(q)$ is the scattering amplitude given by

$$B(q) = \int_0^\infty \Delta\rho(r) \frac{\sin qr}{qr} r^2 dr, \tag{2}$$

where $\Delta\rho(r)$ is the excess radial electron density inside the particles above the solvent. The cores composed of solid polystyrene in water have an excess electron density of 7 e^-/nm^3, whereas the polyelectrolyte layer is modeled by 5 subsequent shells differing in their local excess electron density $\Delta\rho(r)$. For nearly full stretched chains, $\Delta\rho(r)$ decays as r^{-2} [18].

The analysis of the scattering intensity $I(q)$ can be done by dividing the q range into three parts [16]: At lowest q values ($q \leq 0.03$ nm^{-1}) the interaction between the particles in solution, that is $S(q)$ [cf. Eq. (1)] cannot be disregarded. This part of $I(q)$ will be treated further below. At intermediate scattering angles ($0.03 \leq q \leq 0.5$ nm^{-1}) the adsorbed proteins do not manifest as individual units and the uptake of protein essentially increases $\Delta\rho(r)$ [16]. Hence, the term $I_{CS}(q)$ for $q > 0.03$ nm^{-1} can be treated as in the case of unloaded particles. Moreover, Eq. (2) shows that the forward scattering is proportional to the total amount of adsorbed protein which increases from the unloaded system [16]. Finally, at highest q values, the proteins embedded within the polyelectrolyte layer as well as the free protein left in solution may be treated as a system of independent scattering units. Thus, the scattering intensity measured beyond 0.5 nm^{-1} can be modeled by the sum of the scattering intensity $I_0(q)$ of the loaded brush and the intensity of a solution of proteins having the concentration as used in the experiment. The increase in the local $\Delta\rho(r)$ from the unloaded system directly provides the spatial distribution of the BSA within the brush layer with good accuracy [16].

Figure 2 displays the typical evolution of $I(q)$ as a function of time. The gradual uptake of protein can be directly seen from the shift of the side maxima to smaller q values. The decomposition of $I_0(q)$ to different contributions is illustrated for the $t = 0$ curve. In addition, the scattering by the protein is also indicated by the dash-dotted line. The continuous lines depict the modeling of data for $q > 0.03$ nm^{-1} assuming a dispersion of noninteracting polyelectrolyte brushes [$S(q) = 1$, Eq. (1)].

As mentioned above, for a complete description of intensities of bare and loaded brushes for $q < 0.03$ nm^{-1}, the $S(q)$-term needs to be included since electrostatic repulsive interactions lead to a decrease of $I(q)$ at low q region. Polyelectrolyte brushes interact through both steric and electrostatic interactions, and $S(q)$ can be calculated directly from the charge of a single polyelectrolyte brush, its polydispersity, and its concentration by use of integral equation approach (see Ref. [17]). The dotted lines (with the same color) in Fig. 2 show the result of this analysis. The screened Coulomb interaction between the polyelectrolyte brushes was found to be independent of the uptake of the proteins.

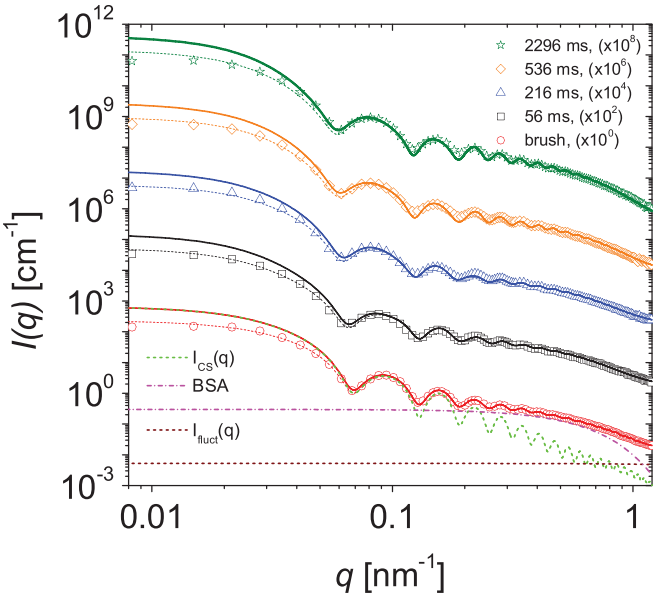

FIG. 2 (color). TR-SAXS intensities as a function of time t. For clarity, the upper curves have been multiplied by the factor indicated in the legend. The solid lines represent SAXS modeling by Eq. (1) with $S(q) = 1$. The dotted lines (same color) depict the calculated intensities with $S(q)$ of a dispersion of interacting SPB obtained from the PRISM-approach [17]. The differences between the dotted and solid lines manifest the repulsive electrostatic interaction between the particles. The lower most curve also illustrates the decomposition of $I_0(q)$ into $I_{CS}(q)$ and $I_{fluct}(q)$ terms and the bulk BSA scattering.

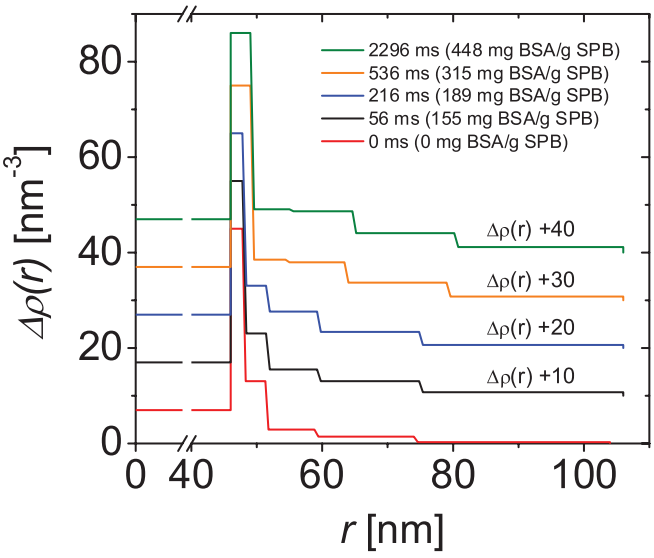

FIG. 3 (color). The excess electron density derived from the analysis presented in Fig. 2 and the corresponding uptake of BSA per SPB is given in the parenthesis. For clarity successive plots have been shifted up by 10 nm^{-3} as indicated in the legend.

Figure 3 displays the local excess electron density $\Delta\rho(r)$ derived from the fits to the SAXS data in Fig. 2. The uptake of BSA into the brush layer is relatively fast and the final stage is reached within 3 seconds. However, the time needed by a single protein molecule to diffuse freely through the shell thickness is less than a millisecond. Hence, the motion of BSA molecules in the brush layer has been slowed down significantly. The difference between the number of electrons in the bare and the loaded brush gives the total amount of adsorbed protein, τ_{ads}. Figure 4 depicts that τ_{ads} increases with time as $t^{1/4}$. This result may at first be an indicative of diffusion in a one-dimensional system [19] as in the reptation model introduced by de Gennes [20]. Another closely related example is the so-called single-file diffusion problem encountered in condensed matter such as one-dimensional hopping conductivity [21], ion transport in biological membranes [22], channeling in zeolites [23], and diffusion of colloidal particles in one-dimensional channels [24]. The main result is that the mean-square displacement $\langle x(t)^2 \rangle$ of individual particles exhibits subdiffusive behavior due to the hindered motion caused by surrounding particles. Individual particles confined to narrow regions are unable to pass each other and the sequence of particles remains the same over the time. As overtaking is excluded, the motion of individual particles requires the collective motion of many other particles leading to the anomalous behavior of the self-diffusion.

The system considered here differs from the channeling experiments mentioned above for several reasons: (a) The proteins do not move inside unconnected one-dimensional pores but through a three-dimensional brush. (b) A recent computer simulation study [25] has demonstrated that both monovalent and trivalent ions move diffusively inside the brush, e.g., the root-mean-square displacement increases

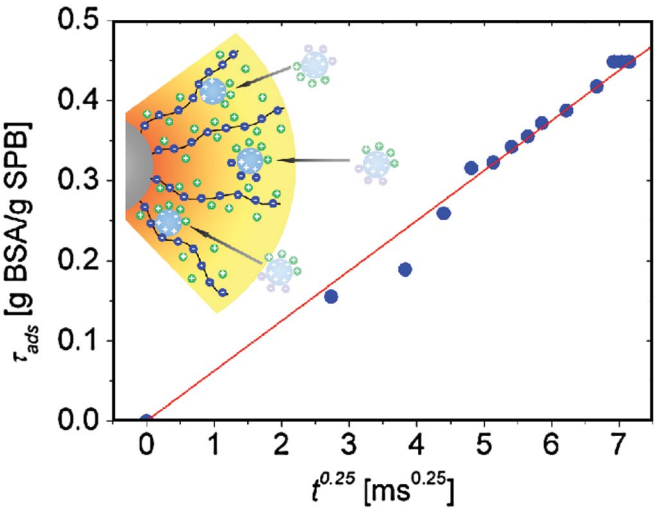

FIG. 4 (color). Overall amount of adsorbed protein, τ_{ads} as a function of time. τ_{ads} has been obtained from the electron density profiles shown in Fig. 3. The inset schematically depicts the motion of proteins through the polyelectrolyte layer in terms of Eqs. (3)–(5). The proteins interact with the polyelectrolyte chains through the positive patches on their surface.

with time as $t^{1/2}$. (c) The observed motion of the proteins is unidirectional in a nonequilibrium state, e.g., the proteins move toward the solid core until the equilibrium state characterized by a maximum uptake has been established.

The observed $t^{1/4}$ behavior for the present system can be understood in terms of a simple model as schematically shown in the inset of Fig. 4. The motion of the proteins within the brush is governed by a balance of frictional and external forces:

$$\zeta \frac{dr(t)}{dt} = -\frac{dU(r)}{dr}, \tag{3}$$

where $r(t)$ is the trajectory of the center of mass of a protein and $U(r)$ is the effective potential acting on a protein. If the protein is modeled as a sphere of radius a, and the viscosity of the solvent is η, then the frictional force is given by $\zeta = 6\pi\eta a$. Within a second virial approach [26] the effective potential $U(r)$ is proportional to the local monomer concentration (cf. Fig. 4). Because of the nearly full stretched polyelectrolyte chains both the monomer density and the local excess electron density scale with r^{-2}. Thus the potential is given by

$$U(r) = \frac{K}{r^2}, \tag{4}$$

where K is a constant. The radial counterion distribution also scales as r^{-2} [18]. The solution of the equation of motion, [Eq. (3)] with [Eq. (4)] is given by

$$r(t) = \left(\frac{8Kt}{\zeta}\right)^{1/4}. \tag{5}$$

Hence, the unidirectional displacement of individual proteins and the total amount of adsorbed proteins increases with time as $t^{1/4}$ as shown in Fig. 4.

In conclusion, we have demonstrated that proteins undergo a directed motion within the spherical polyelectrolyte brush layer. This leads to a subdiffusive behavior and the total amount of adsorbed protein scales with $t^{1/4}$. Evidently, this finding has a general application to the diffusion of proteins through layers of charged polymers. It demonstrates that the self-organization of proteins within charged tethered polymer layers is governed by directed motion. Hence, the analysis presented here could be used to estimate the characteristic time for protein diffusion in more complex environments such as ion exchange chromatography. Similar directed motions of proteins and other biomolecules through biological membranes could play a pivotal role in their self-assembly.

Financial support by the Deutsche Forschungsgemeinschaft within ESF-BIOSONS and SFB 481, Bayreuth, is gratefully acknowledged.

*Matthias.Ballauff@uni-bayreuth.de

[1] *Physical Chemistry of Biological Interface*, edited by A. Baskin and W. Norde (Marcel Dekker, New York, 1999).
[2] C. Czeslik, Z. Phys. Chem. **218**, 771 (2004).
[3] W. Senaratne, L. Andruzzi, and C. K. Ober, Biomacromolecules **6**, 2427 (2005).
[4] A. Toscano and M. M. Santore, Langmuir **22**, 2588 (2006).
[5] J. Ståhlberg, J. Chromatogr. A **855**, 3 (1999).
[6] K. L. Prime and G. M. Withesides, Science **252**, 1164 (1991).
[7] J. H. Lee, H. B. Lee, and J. H. Andrade, Prog. Polym. Sci. **20**, 1043 (1995).
[8] D. S. Salloum and J. B. Schlenoff, Biomacromolecules **5**, 1089 (2004).
[9] J. Dai, G. L. Baker, and M. L. Bruening, Anal. Chem. **78**, 135 (2006).
[10] A. Kusumo, L. Bombalski, Q. Lin, K. Matyjaszewski, J. W. Schneider, and R. D. Tilton, Langmuir **23**, 4448 (2007).
[11] L. E. Valenti, P. A. Fiorito, C. D. García, and C. E. Giacomelli, J. Colloid Interface Sci. **307**, 349 (2007).
[12] A. Wittemann and M. Ballauff, Phys. Chem. Chem. Phys. **8**, 5269 (2006).
[13] B. R. Young, W. G. Pitt, and S. L. Cooper, J. Colloid Interface Sci. **125**, 246 (1988).
[14] M. Ballauff, Prog. Polym. Sci. **32**, 1135 (2007).
[15] P. Panine, S. Finet, T. Weiss, and T. Narayanan, Adv. Colloid Interface Sci. **127**, 9 (2006).
[16] S. Rosenfeldt, A. Wittemann, M. Ballauff, E. Breininger, J. Bolze, and N. Dingenouts, Phys. Rev. E **70**, 061403 (2004).
[17] L. Harnau and J.-P. Hansen, J. Chem. Phys. **116**, 9051 (2002).
[18] N. Dingenouts, M. Patel, S. Rosenfeldt, D. Pontoni, T. Narayanan, and M. Ballauff, Macromolecules **37**, 8152 (2004).
[19] E. Levine, D. Mukamel, and G. M. Schütz, Europhys. Lett. **70**, 565 (2005).
[20] P. G. de Gennes, J. Chem. Phys. **55**, 572 (1971).
[21] P. M. Richards, Phys. Rev. B **16**, 1393 (1977).
[22] E. Neher, Science **256**, 498 (1992).
[23] K. Hahn, J. Kärger, and V. Kukla, Phys. Rev. Lett. **76**, 2762 (1996).
[24] C. Lutz, M. Kollmann, and C. Bechinger, Phys. Rev. Lett. **93**, 026001 (2004).
[25] Y. Mei, K. Lauterbach, M. Hoffmann, O. V. Borisov, M. Ballauff, and A. Jusufi, Phys. Rev. Lett. **97**, 158301 (2006).
[26] J.-P. Hansen and I. R. McDonald, *Theory of Simple Liquids* (Academic, London, 1986).